

CONF-830805--34

CONF-830805--34

DE83 010571

Analysis of HCDA Loads and Containment Response of
a Large Loop-Type LMFBR

C. Y. Wang, W. R. Zeuch, Y. W. Chang, S. H. Fistedis
Reactor Analysis and Safety Division
Argonne National Laboratory
9700 South Cass Avenue
Argonne, Illinois 60439, U.S.A.

The submitted manuscript has been authored
by a contractor of the U. S. Government
under contract No. W-31-109-ENG-38.
Accordingly, the U. S. Government retains a
nonexclusive, royalty-free license to publish
or reproduce the published form of this
contribution, or allow others to do so, for
U. S. Government purposes.

DISCLAIMER

This report was prepared as an account of work sponsored by an agency of the United States Government. Neither the United States Government nor any agency thereof, nor any of their employees, makes any warranty, express or implied, or assumes any legal liability or responsibility for the accuracy, completeness, or usefulness of any information, apparatus, product, or process disclosed, or represents that its use would not infringe privately owned rights. Reference herein to any specific commercial product, process, or service by trade name, trademark, manufacturer, or otherwise does not necessarily constitute or imply its endorsement, recommendation, or favoring by the United States Government or any agency thereof. The views and opinions of authors expressed herein do not necessarily state or reflect those of the United States Government or any agency thereof.

MASTER

DISTRIBUTION OF THIS DOCUMENT IS UNLIMITED

As part of a comprehensive safety study, analyses are presented on the hydrodynamic loads and containment response of a large loop-type LMFBR subjected to an HCDA of a 1000 MW energy release. The reference reactor consists of a primary vessel, a head cover, and various complex internals such as the upper internal structure (UIS), the core-support structure (CSS), radial shield, shield baffles, and deflector plate. Three calculations are performed with the ANL hybrid Lagrangian-Eulerian containment code, ALICE-II. They deal, respectively, with: (1) the calculation of HCDA hydrodynamics, reactor-cover loads, and forces on the UIS; (2) investigating the mitigating effect of the UIS on the cover loading as well as the containment response; and (3) the analysis of overall containment integrity, including interaction of fluids with the deformable UIS and CSS.

Our first calculation on the hydrodynamics shows that a small plastic strain of 1.11% takes place at the upper vessel. A typical pressure history underneath the cover consists of three distinct pulses. A sharp peak due to the slug impact occurs first, followed by two longer, steadier pulses due mainly to the wave reflection from the deformed vessel and the residual pressure in the moving fluids. The maximum peak value is about 26 MPa. Forces acting on the UIS assembly and the deflector plate are comprised of contributions from incident-wave propagation and the reflection from slug impact, respectively. Maximum values of these two forces are 350 and 140 MN, respectively.

The second ALICE-II calculation, the UIS parametric study, reveals that the UIS plays a substantial role in mitigating the slug-impact loads as well as in reducing the upper vessel deformation. The peak impact pressure and the vessel deformation are 26 MPa and 7.90 cm with the UIS present, compared to 70 MPa and 17.49 cm without the UIS.

Results from the third calculation, dealing with the integrated containment analysis, indicate that deformations of the upper vessel, core barrel, radial shield, the UIS, and the bottom vessel are all small. However, the axial displacement of the CSS is quite large, having a value of 64 cm. We have also found from a comparison of the first and the third calculations that the cover loads obtained from the case 1 calculation are conservative.

The analyses presented in this paper represent a variety of parametric calculations providing useful guidance for subsequent design decisions. Special emphasis must be given to the importance of the UIS in reducing the effects of energy releases on the reactor cover region; and attention must be given to the core support structure, due to its complex structural response, and its potential for energy absorption.

1. Introduction

Analyses are presented on the hydrodynamic loads and containment response of a large loop-type LMFBR subjected to an HCDA. The reference reactor considered here consists of a reactor vessel, a vessel head, and a variety of complex internals, including the upper internal structure (UIS) and the core-support structure (CSS). In order to provide a comprehensive evaluation of the LMFBR structural capabilities to accommodate loads from events beyond the design basis, several objectives were established. These objectives were: (1) to calculate head loads, forces on the UIS, and hydrodynamics from one HCDA energetic source; (2) to investigate the effect of the UIS on the slug impact and containment response; (3) to analyze containment integrity, including interaction of fluids with all the structural components; (4) to utilize head loads to calculate the head response of the reference reactor; and (5) to compute the detailed UIS component response using the UIS forces.

To fulfill these objectives we decided to choose the advanced arbitrary Lagrangian Eulerian containment code, ALICE-II [1-3], for the hydrodynamic and containment analyses, and to employ the finite element codes NEPTUNE and SAFE/RAS for calculating, respectively, the detailed cover and UIS responses. This paper deals with the ALICE-II calculations established in objectives (1)-(3). Detailed analyses of the reactor head and the UIS responses will be reported in two companion papers at this conference [4,5].

Three calculations are performed with the ALICE-II code. The first calculation is intended to provide conservative head loadings and UIS forces utilized in objectives (4) and (5), and hence treats the UIS and CSS as rigid. The second calculation deals with a UIS parametric study in which the UIS was not considered in the mathematical model. The third calculation deals with an integrated containment analysis where the UIS and CSS are treated as deformable structures in accordance with their initial designs. The HCDA energy source has a total energy content of 1000 MJ.

We will proceed to describe the model used in the analyses as well as the results obtained from various ALICE-II calculations.

2. Description of Models

The reactor configuration and the preliminary design of the core-support structure are shown in Figs. 1 and 2, respectively.

The mathematical model used in the first two ALICE-II analyses of the LDP reactor is shown in Fig. 3. It consists of a reactor core, the core barrel, radial shield, shield barrel, core-support structure, upper internal structure (UIS), deflector plate, baffle plates, and the reactor vessel. In the analysis, the core barrel, radial shield, shield barrel, baffle plates, and reactor vessel are treated as deformable structures. The core-support structure is treated as a rigid structure supported by a deformable skirt. The UIS is connected to the reactor head through connecting columns. The openings in the UIS are lumped into two annular holes which have the same area as the actual holes in the UIS. The deflector plate and the UIS are modeled as rigid obstacles which will transmit loads directly to the reactor head through the UIS supporting columns.

Note that in the case 1 calculation the supporting columns are assumed to be rigid. By assuming the UIS and the core-support structure to be rigid, conservative head loadings were obtained for the reactor-cover analysis. Also note that in the case 2 calculation the UIS, UIS columns, and the deflector plate are completely removed.

The mathematical model utilized in the third ALICE-II calculation, dealing with an integrated containment analysis, is shown in Fig. 4. In this analysis the UIS assembly is treated as a perforated and movable structure, but nondeformable. However, the UIS supporting columns are modeled as deformable structures by 3-D pipe elements. The imperfections of the UIS columns were simulated by displacing the original coordinates of the structural nodes laterally. Modeling of the CSS presents some difficulties for the ALICE-II code because of the design complexity, as shown in Fig. 2, in addition to the 3-D nature of its response. For simplicity, the CSS is simulated by the 2-D axisymmetric shell elements.

3. Results

3.1 Case 1 (Rigid UIS and CSS): Hydrodynamic and Cover-Loading Calculation

Figure 5 presents reactor configurations at three different times. These configurations show how the core-gas bubble expands and deforms as it encounters the sharp corners of the structural components. Due to the presence of the deflector plate, the coolant slug impact on the reactor cover occurs first in the side zones away from the center. As a result, the cover gas is trapped in the region near the center line. Furthermore, these configurations reveal the location and magnitude of the permanent deformation of the primary vessel occurring during the course of the excursion.

The pressure history in each zone underneath the reactor cover together with the upward and downward forces acting on the UIS and the deflector plate are stored on tape and are used as the input loadings for the three-dimensional reactor-cover analysis. Because of the space limitation only one pressure loading is presented. Figure 6 depicts the pressure history in zone 9 (see Fig. 3 for its location). This pressure loading consists of three types of pulses during the 238 ms of calculation time. The first one, a sharp peak, which has a peak magnitude of 26 MPa occurring at 72 ms, is due to the slug impact. The second, a longer, steadier loading, is due to the residual slug pressure occurring after the vessel wall has deformed to its maximum position. This pulse has a peak value about 12 MPa occurring at 75 ms after the excursion. The third pulse, which has a magnitude of 4 MPa and occurs after 190 ms, is again due to the residual pressure in the moving fluid. This residual pressure is expected to exist in the fluid for a period of time until it is dissipated in the fluid.

Figure 7 depicts the upward force on the UIS assembly as a function of time.

The radial strain as a function of time at vessel node A (see Fig. 3), is given in Fig. 8. It can be seen that the vessel at that position responds plastically. The permanent strain is about 1.11%, which corresponds to a displacement of 7.09 cm. Also, the results given in Fig. 9 indicate that the core-barrel movement is very small and its strain is in the elastic range.

3.2 Case 2 (no UIS, no Deflector Plate): UIS Parametric Calculation

A second calculation, case 2, has been performed with the ALICE-II code to study the primary containment response when the UIS and deflector plate are not included in the mathematical model. The purpose of this calculation is to study the effects of these upper internal structures on the core energy release as well as on the deformation of the vessel wall.

Figure 10 shows reactor configurations at three different times. These configurations indicate that due to the absence of the UIS and deflector plate the slug impact occurs first in the central region while the core gas was trapped in an annular region near the side of the upper containment.

A comparison of case 1 (with UIS and deflector plate) and case 2 (no UIS, no deflector plate) calculations shows that the upper vessel deformation has increased substantially, from 1.16% in the case with UIS, to 2.75% in the case without the UIS. Also, comparison of pressures in a typical zone (zone 9, see Fig. 3) revealed that, in the case of no UIS, the slug impact occurs at a much earlier time. The peak pressure generated by the slug impact has a value of 70 MPa for the case without the UIS, compared to 25 MPa for the case with the UIS. These findings suggest that in the reactor configuration considered here the UIS plays a substantial role in mitigating the slug impact load as well as in reducing the upper vessel deformation.

Note from Fig. 11 that the pressures under the reactor cover have three distinct peaks during the 250 ms of calculation time. The first peak is due to the slug impact which has a magnitude of 70 MPa occurring at 50-55 ms. The second peak is due to the residual slug pressure occurring after the vessel wall has deformed to its maximum position. This pressure peak is about 18 MPa occurring at 135 ms after the excursion. The third pressure peak is again due to the residual pressure in the moving fluid, which has a magnitude of 15 MPa and occurs at 235 ms of time. These pressures are expected to exist in the fluid for a period of time until they are dissipated in the form of strain energy to the vessel wall and thermal energy in the fluid.

3.3 Case 3 (Deformable UIS and CSS): Preliminary Integrated Fluid-Structure Interaction Analysis

Primary containment normally consists of complicated internal components such as the UIS and CSS. Two methods can be utilized to analyze their dynamic response during an HCUA. The first one is the conventional, decoupled, two-step calculation which ignores fluid-structure interaction. More specifically it uses: (1) a containment code to calculate the force histories on the UIS and CSS, assuming that these components are rigidly fixed in space; and (2) the calculated forcing function as input to the three-dimensional code to compute the detailed structural response. The second method, on the other hand, accounts for the fluid-structure interaction, but models these structures in a simplified manner.

Here, we present the calculation which treats the UIS and CSS as deformable. In the analysis the CSS is modeled as an axisymmetric structure using plate and shell elements. The thickness of the top and bottom plates are increased to account for the rigidity of the support I-beams used in the actual design.

By comparing the results of case 1 and case 3 calculations, our aim is: (a) to study the conservatism of the head loading obtained from the case 1 calculation, and (b) to provide a scoping analysis on the deformation of the UIS and CSS. Since this CSS model may deviate from the actual structural design, the analysis presented here is preliminary in nature.

Figure 12 gives reactor configurations at several times. Figure 13 provides a pressure history at zone 9 (see Fig. 4 for its location) underneath the cover. Because certain amounts of energy have been transformed into strain energy of the UIS and CSS, the upper vessel deformation and the peak slug-impact loading are smaller than the corresponding values of the case 1 calculation. Our results show that the upper vessel deformation and peak loading are 6.59 cm and 22 MPa for the case 3 (deformable UIS and CSS) calculation, compared to 7.09 cm and 26 MPa for the case 1 calculation. The difference is 7% less for vessel deformation and 15% less for peak loading. We also observed from the case 3 calculation that

the downward displacement of the CSS is quite large, having a value of 64 cm. Therefore, a detailed 3-D analysis of the CSS should be performed.

4. Conclusion

The analyses given in this paper represent a variety of parametric calculations, which not only provide a basic understanding of complex physical phenomena involved during an HCDA, but also give useful guidance for subsequent design iterations to accommodate these accident loads. From the results of this study several specific conclusions can be drawn: (a) the primary containment of the reference reactor considered here can withstand the HCDA of a 1000 MW energy release. The strain and deformation of the primary vessel are small. (b) Deformations of the core barrel, radial shield, skirt, and the UIS are also small. (c) The UIS plays a substantial role in mitigating the slug impact loads. (d) The axial displacement of the CSS is quite large. Therefore, a detailed 3-D analysis of this complex structure should be performed. (e) The computed cover loads and UIS forces are conservative. Therefore, the forcing functions used in the 3-D analysis of the cover and UIS response given in two companion papers [4,5] are conservative. X

5. Acknowledgments

This work was performed in the Engineering Mechanics Program of the Reactor Analysis and Safety Division at Argonne National Laboratory, under the auspices of the U.S. Department of Energy.

References

- [1] WANG, C. Y., ZEUCH, W. R., "ALICE-II: An Arbitrary Lagrangian-Eulerian Code for Containment Analysis with Complex Internals," *Trans. Am. Nucl. Soc.*, Vol. 41, p. 364 (June, 1982).
- [2] WANG, C. Y., ZEUCH, W. R., "A Multi-Dimensional Arbitrary Lagrangian Eulerian Method for Dynamic Fluid-Structure Interaction," in *Fluid-Transients and Fluid/Structure Interaction*, eds., Y. W. Shin, F. J. Moody, M. F. Au-Yang, 1982 ASME Special Publication PVP-64, Book No. H00221, pp. 289-316 (June, 1982).
- [3] WANG, C. Y., ZEUCH, W. R., "Recent Developments of the Arbitrary Lagrangian-Eulerian Containment Code ALICE-II," *Trans. 7th Int'l. Conf. on Structural Mechanics in Reactor Technology*, paper E 4/8, Chicago, IL (August, 1983).
- [4] KULAK, R. F., FIALA, C., "Dynamic Response of a Large Loop-Type LMFBR Head Closure to HCDA Loads," *Trans. 7th Int'l. Conf. on Structural Mechanics in Reactor Technology*, paper E 1/8, Chicago, IL (August, 1983).
- [5] KENNEDY, J. M., BELYTSCHKO, T. B., "Mechanical Interactions of UIS Support Columns," *Trans. 7th Int'l. Conf. on Structural Mechanics in Reactor Technology*, paper E 3/1, Chicago, IL (August, 1983).

FIGURE CAPTIONS

1. Configuration of a Large Loop-Type LMFBR
2. Typical Design of the Core-Support Structure
3. Mathematical Model for the Hydrodynamic and UIS Parametric Study
4. Mathematical Model for the Integrated Containment Analysis
5. Reactor Configurations at Three Different Times (Case 1: Hydrodynamic Calculation)
6. Pressure History in Zone 9 Underneath the Reactor Cover (Case 1: Hydrodynamic Calculation)
7. Upward Force on the UIS Assembly as a Function of Time (Case 1: Hydrodynamic Calculation)
8. Radial Strain as a Function of Time at Vessel Node A (Case 1: Hydrodynamic Calculation)
9. Core Barrel Strain as a Function of Time (Case 1: Hydrodynamic Calculation)
10. Reactor Configurations at Three Different Times (Case 2: no UIS)
11. Pressure History in Zone 9 Underneath the Reactor Cover (Case 2: no UIS)
12. Reactor Configurations at Three Different Times (Case 3: Integrated Containment Analysis)
13. Pressure History in Zone 9 Underneath the Reactor Cover (Case 3: Integrated Containment Analysis)

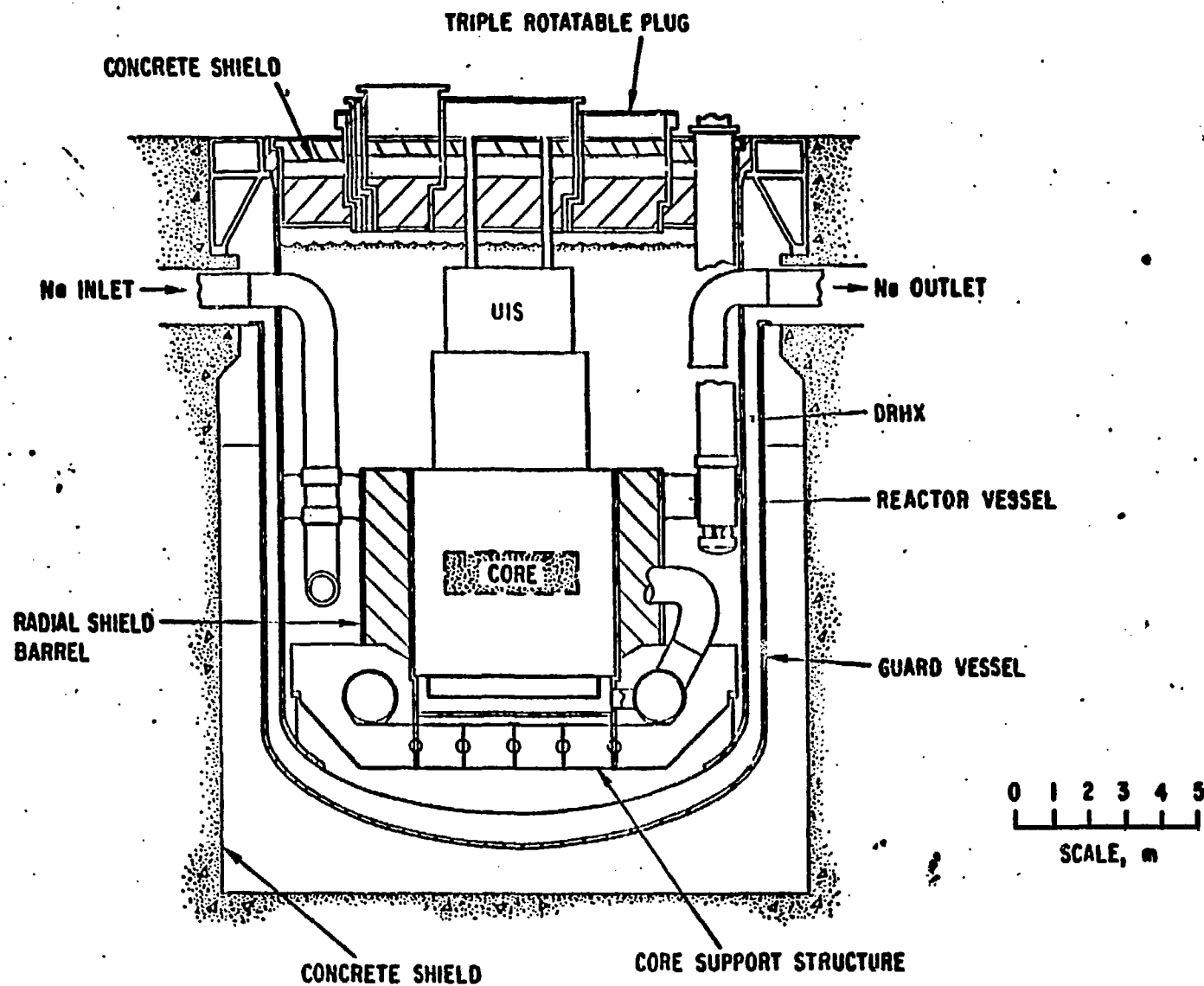


Fig. 1. Configuration of a Large Loop-Type LMFBR

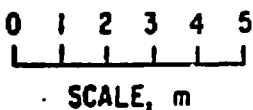
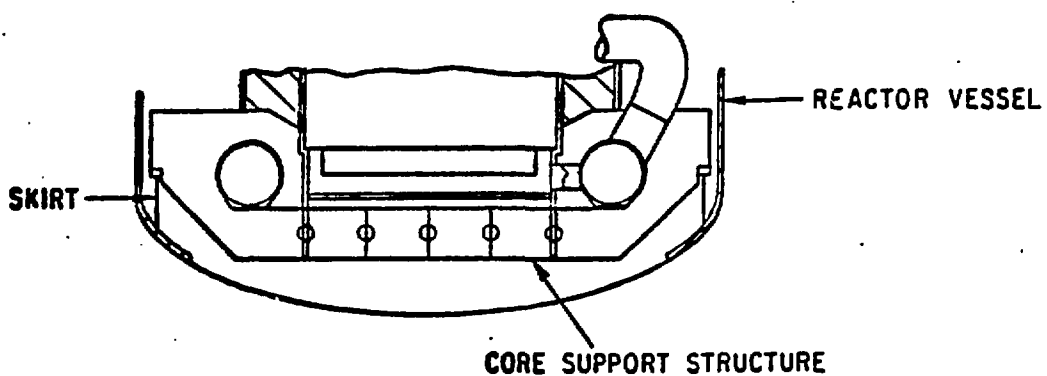
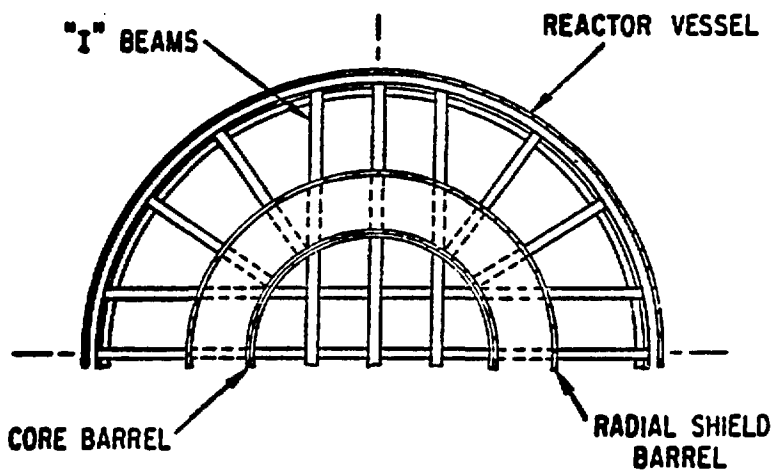


Fig. 2 Typical DESIGN of the "Core-support structure"

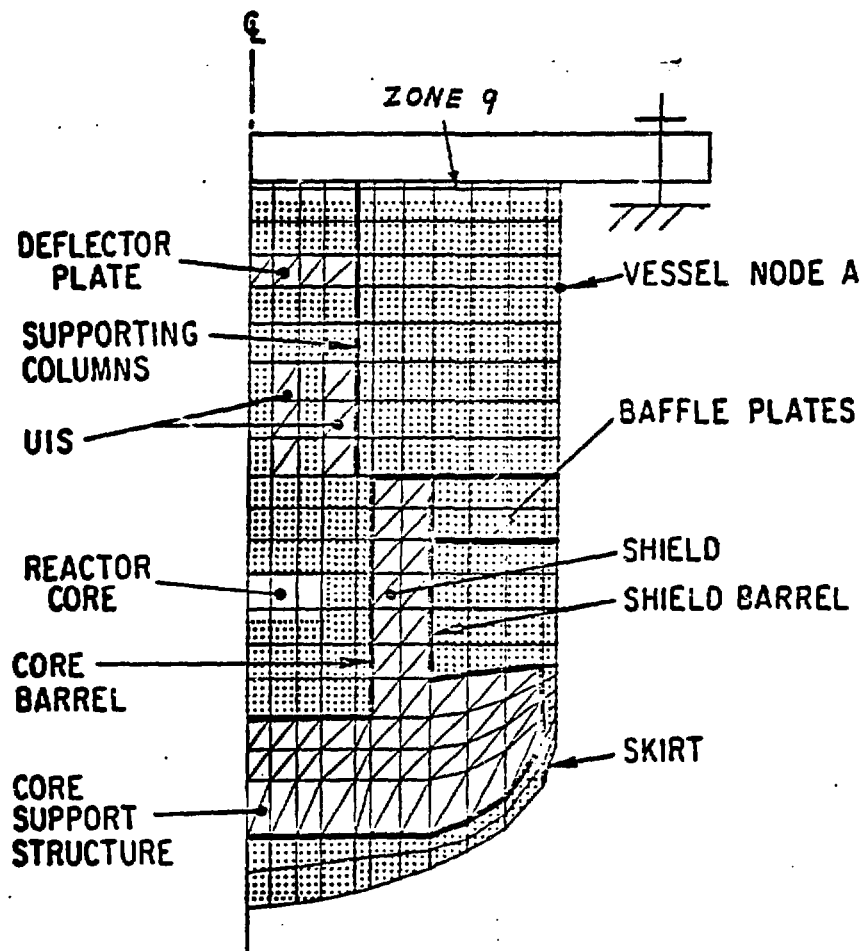


Fig 3. Mathematical Model for the Hydrodynamic and UIS Parametric Study

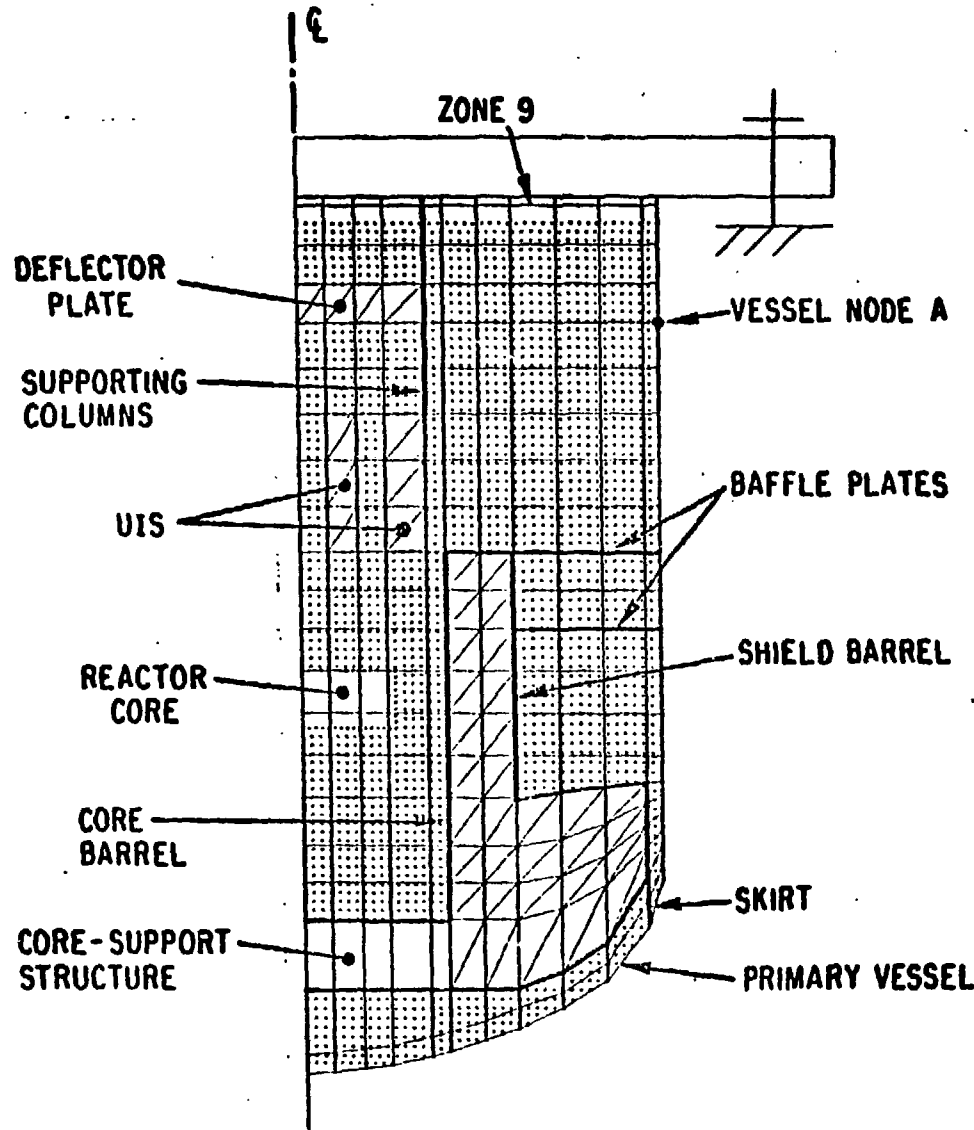


Fig. 4. Mathematical Model for the Integrated Containment Analysis

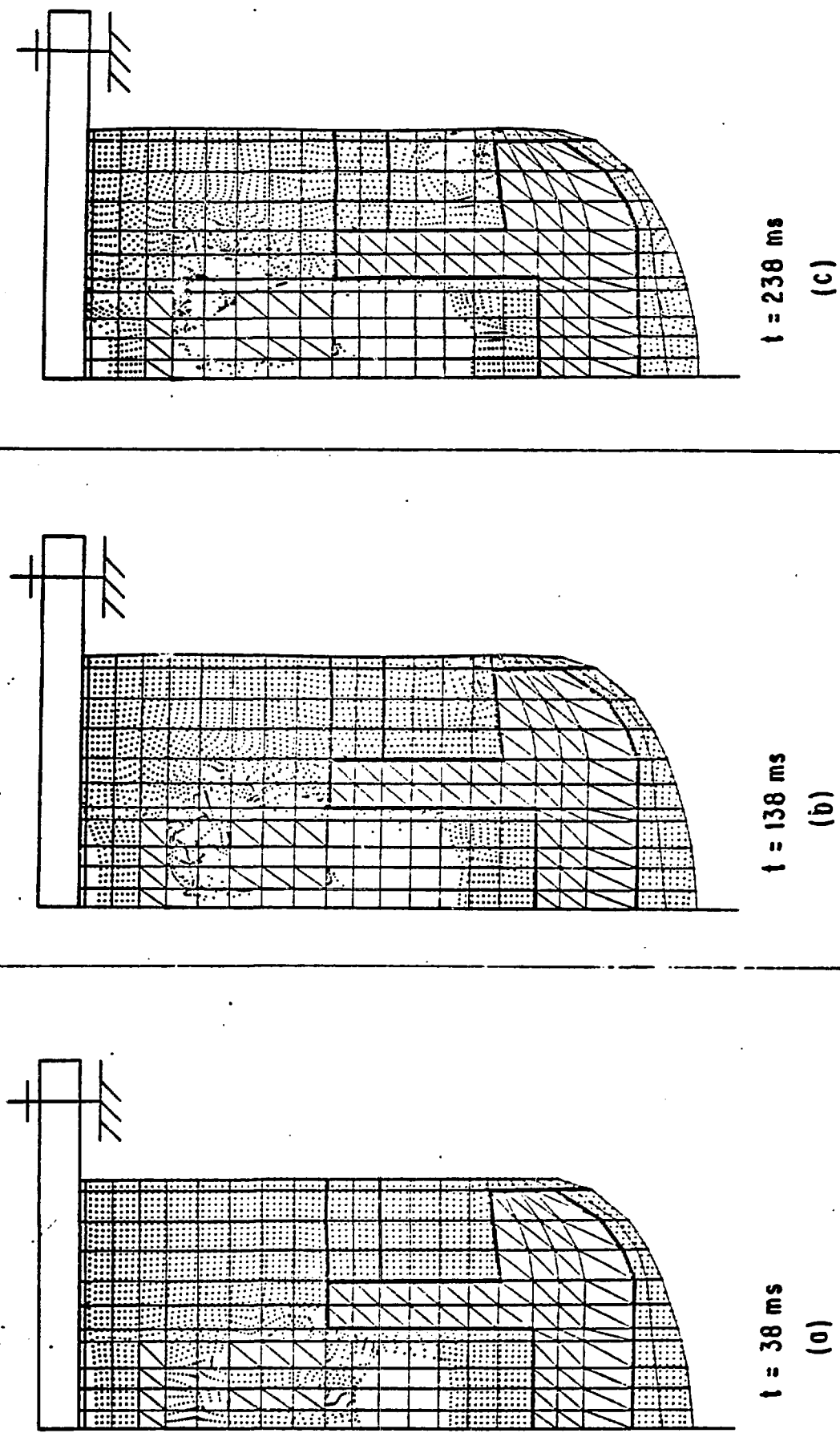


Fig. 5. Reactor Configurations at Three Different Times (Case 1: Hydrodynamic Calculation)

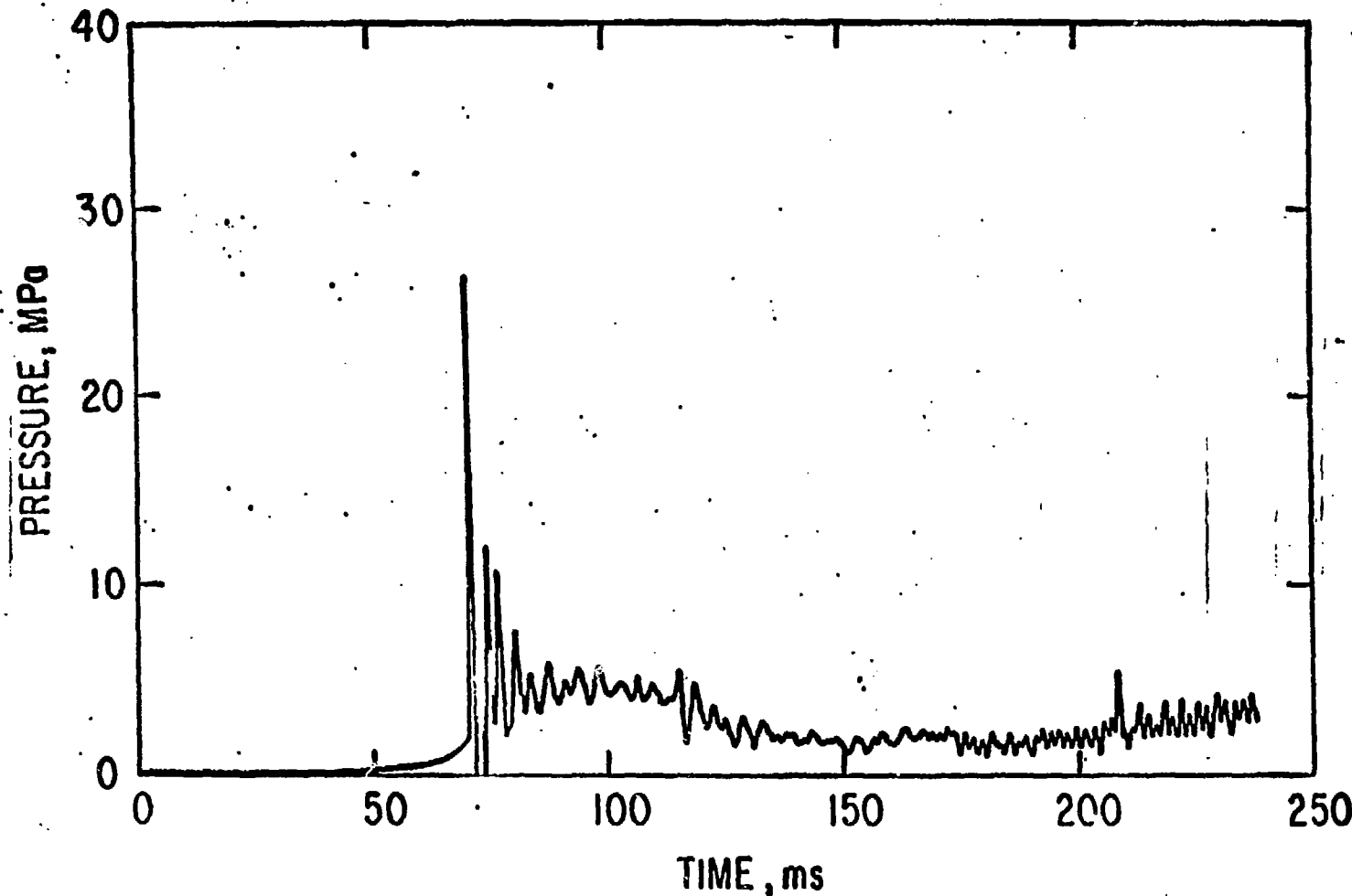


Fig. 6. Pressure History in Zone 9 Underneath the Reactor Cover (Case 1:
Hydrodynamic Calculation)

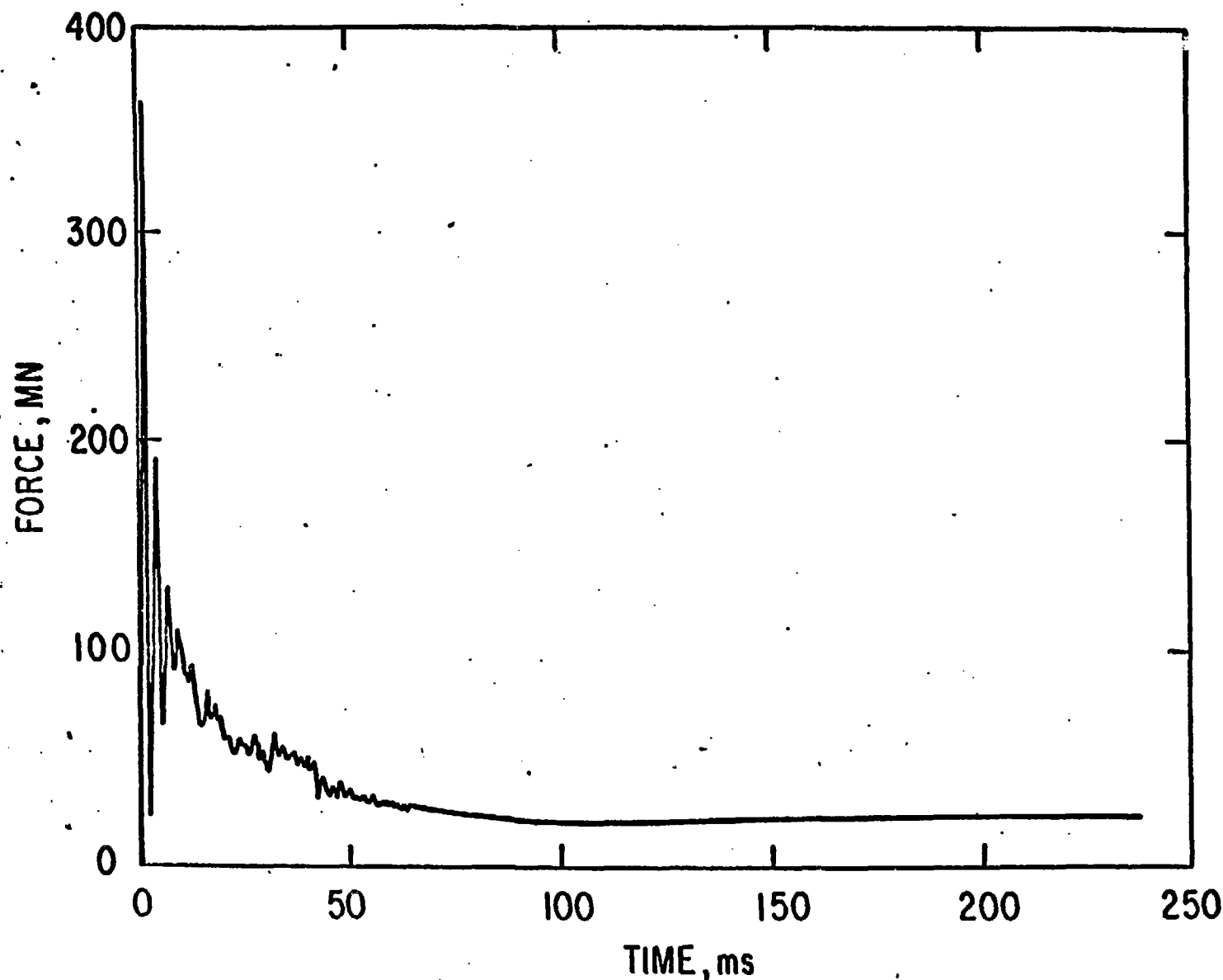


Fig. 7. Upward Force on the UIS Assembly as a Function of Time (Case 1: Hydrodynamic Calculation)

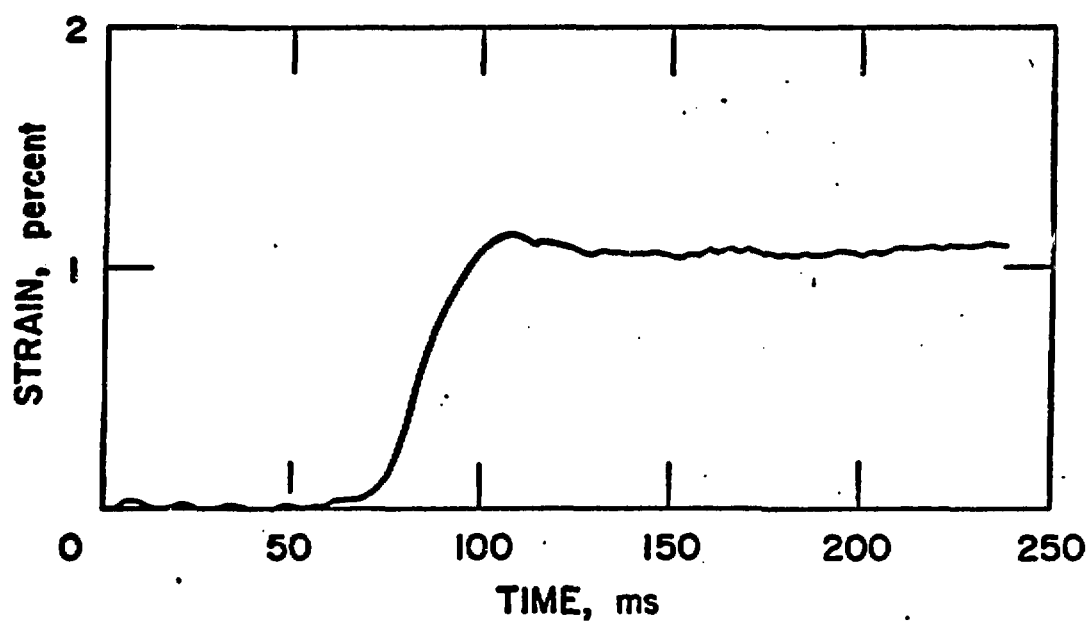


Fig. 8. Radial Strain as a Function of Time at Vessel Node A (Case 1:
Hydrodynamic Calculation)

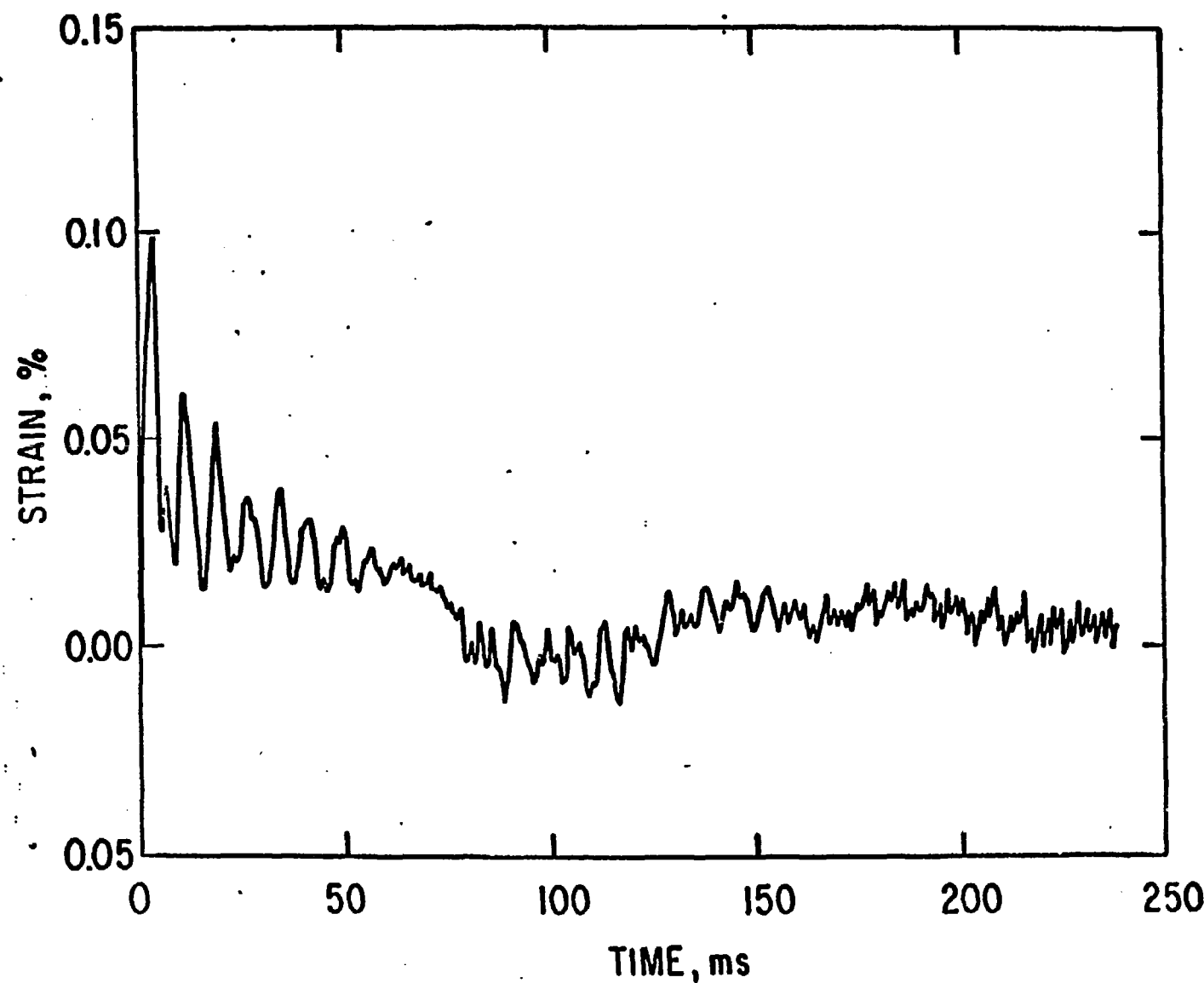
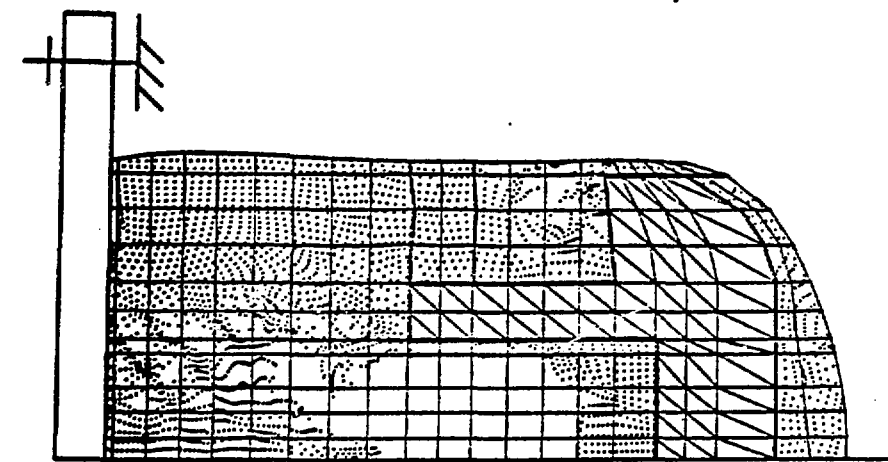
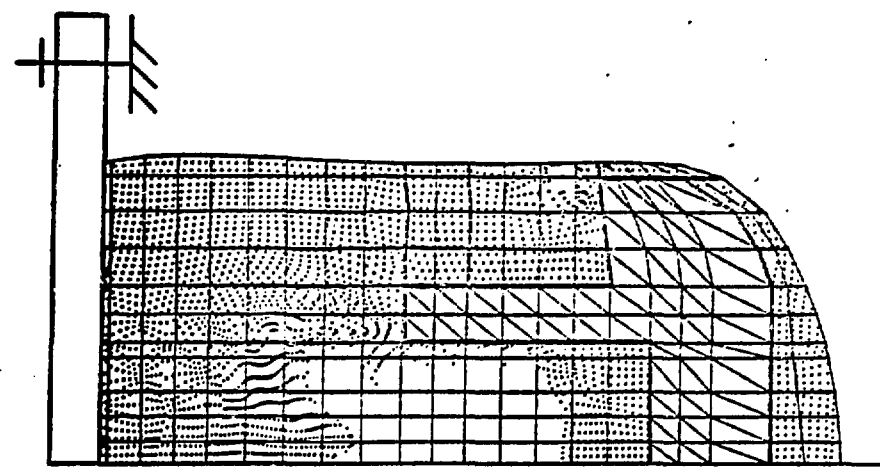


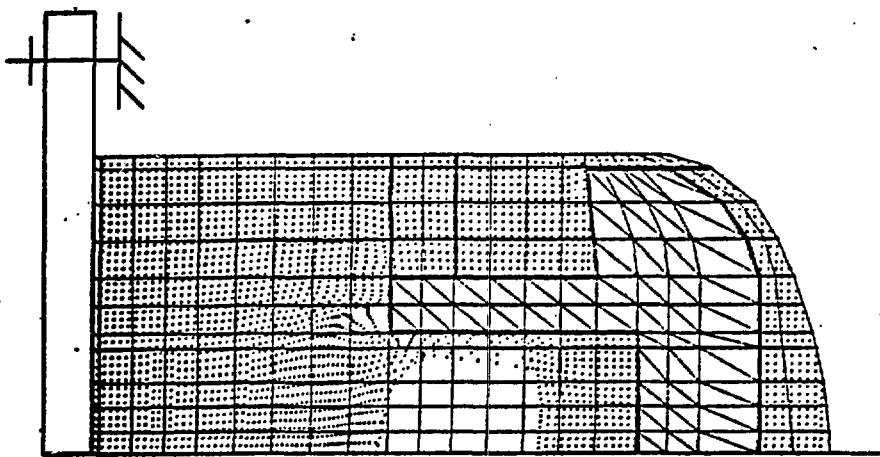
Fig. 9. Core Barrel Strain as a Function of Time (Case 1: Hydrodynamic Calculation)



$t = 238 \text{ ms}$
(c)



$t = 138 \text{ ms}$
(b)



$t = 38 \text{ ms}$
(a)

Fig. 10. Reactor Configurations at Three Different Times (Case 2: no UIS)

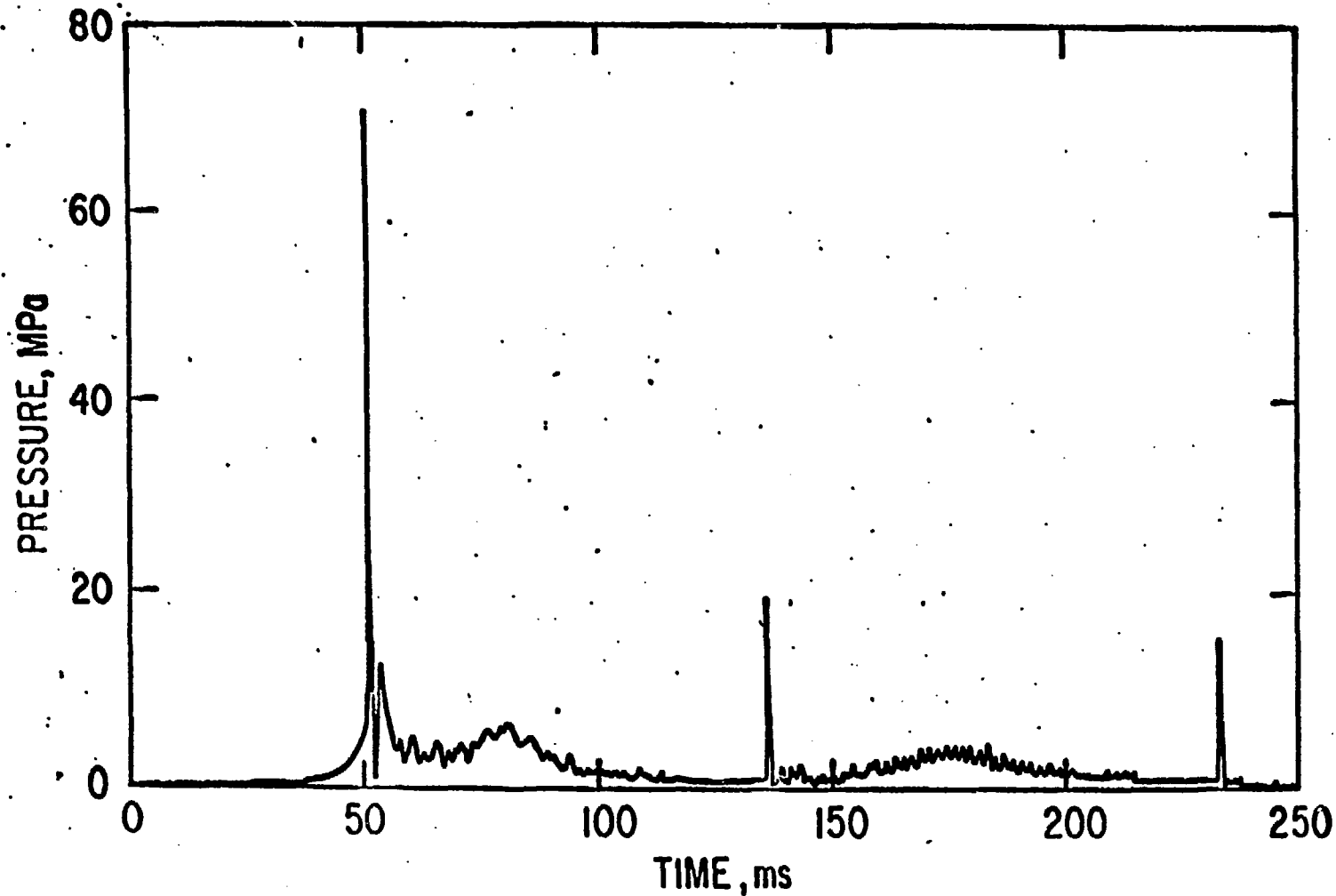
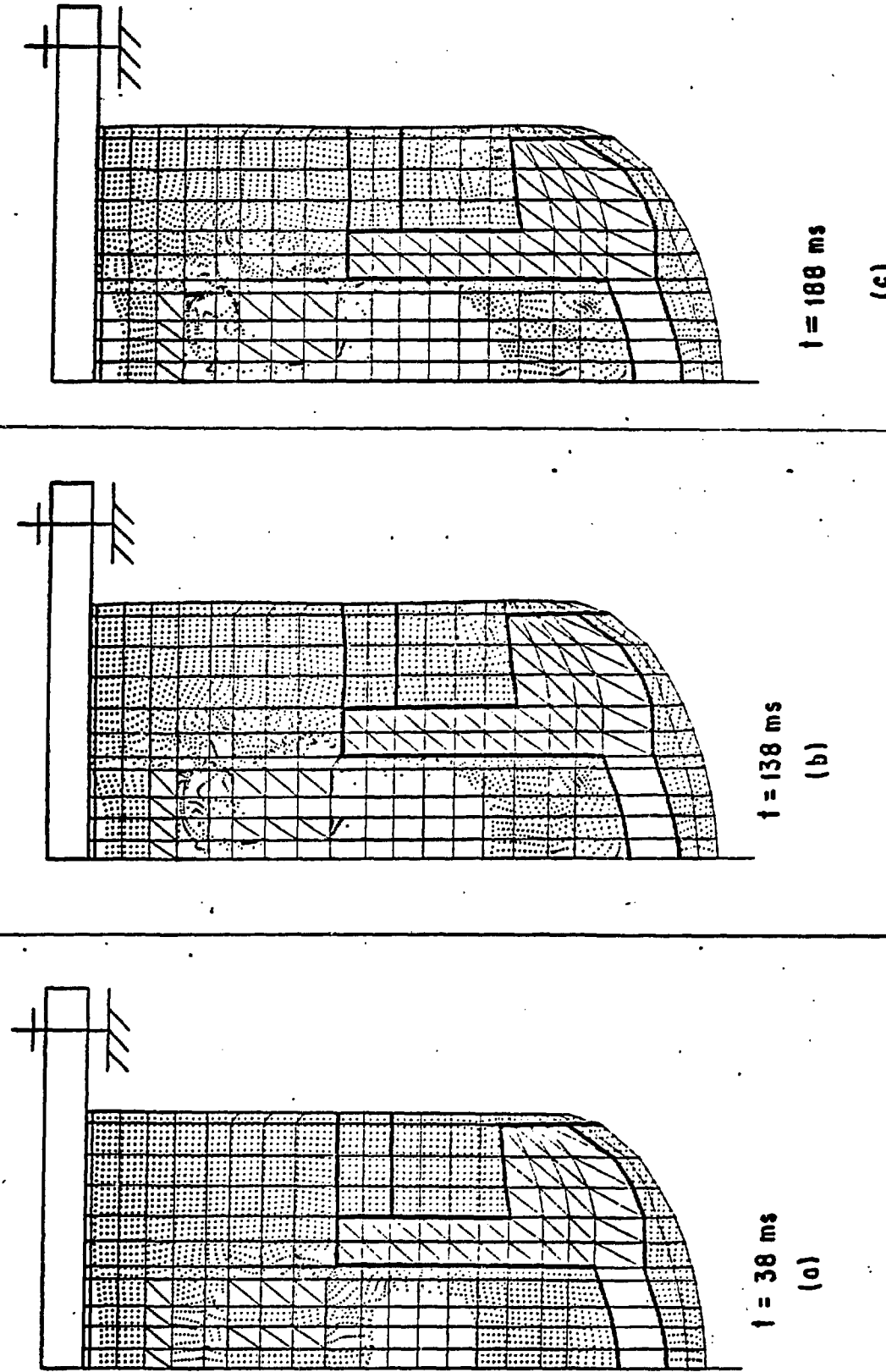


Fig. 11. Pressure History in Zone 9 Underneath the Reactor Cover (Case 2: no UIS)

Fig. 12. Reactor Configurations at Three Different Times (Case 3: Integrated Containment Analysis)



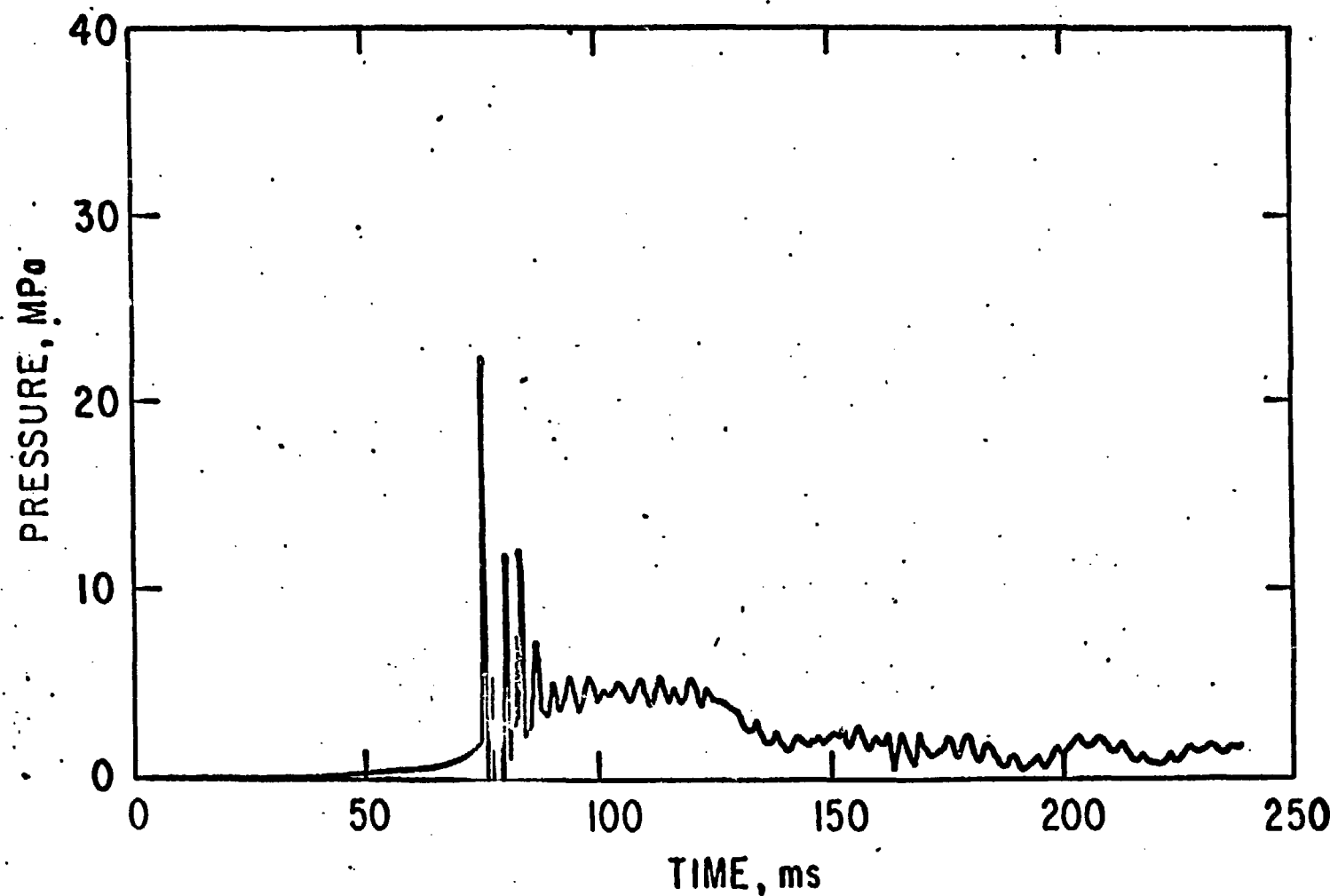


Fig. 13. Pressure History in Zone 9 Underneath the Reactor Cover (Case 3: Integrated Containment Analysis)